Seismic Assessment and Retrofitting of an Old Reinforced Concrete Building in the City of Lisbon

Miguel Afonso
miguel.c.afonso@ist.utl.pt
Instituto Superior Técnico, Universidade de Lisboa, Portugal, 2017

ABSTRACT: History shows that the consequences of a seismic event depend heavily on the vulnerability of constructions. As recognized by several authors, the research in earthquake engineering field should be targeted to the assessment and retrofitting of existing constructions, in order to mitigate the impacts of such event, acting on the vulnerability of existing structures. Motivated by the need to reduce the seismic risk of buildings to acceptable levels, this study addresses the analysis and retrofitting of a reinforced concrete (RC) wall-frame building in the city of Lisbon, considered as representative of the building stock between 1960 and 1980. These typical old RC buildings, design without an appropriate seismic design criterion, represent an identified source of risk. The main goals of this work are to identify and quantify the expected deficiencies of the structure, in order to propose a retrofitting strategy, with the aim on fulfil the seismic performance requirements in Part 3 of Eurocode 8, by means of non-linear static analysis of an 3D model of the structure developed in the software SAP2000. It was considered the N2 method, as prescribed by Eurocode 8, complemented with the extended N2 method, which considers the effect of the torsional behaviour of plan-asymmetric structures and the effects of higher modes of vibration. A sensitivity analysis is performed to assess the influence of the infill walls and the non-linear modelling strategies for the RC-wall. Based on the conclusions of the seismic analysis of the building, a proposal for the retrofitting is presented and analysed.

Keywords: *earthquake engineering, reinforced concrete building, seismic assessment, seismic retrofitting, nonlinear static analysis, Part 3 of Eurocode 8, N2 method, Extended N2 method, structural modelling, SAP2000 software*

1. INTRODUCTION

In Portugal, the relatively low statistic rate of major earthquakes could explain the way in which the society leads with the seismic risk. However, the catastrophic consequences of such event, mostly due to a higher seismic vulnerability of the existing buildings, should not be underestimated.

The seismic vulnerability of the building could be correlated to the time of construction and the respective standards at the time. The first Portuguese norm to explicit consider seismic resistance was the *Regulamento de Segurança das Construções contra Sísmos* [1], and was only implemented in 1958. This first approach to the seismic design of buildings was based on simplified design methods, considering the seismic action as static equivalent lateral forces. However, this simplified seismic design methodology of structures, combine with several inadequate structural design options, namely in terms of control of brittle failure of elements and inadequate design regarding the ductile behaviour of the structural components, lead in general to a poor seismic performance of the building. According to [2] the seismic performance of buildings built in Portugal between 1960 and 1980 are well below 50% of the seismic demand of the actual seismic standards. In 1983, with the implantation of the *Regulamento de Estruturas de Betão Armado e Pré-Esforçado* [3] the seismic performance of buildings increased substantially, mostly due to introduction of several ductile detailing rules. Nowadays, after years of experience accumulated in the field of seismic engineering, the seismic resistance design adds very little to the construction cost of a new building. On the other hand, the seismic retrofitting cost of old existing buildings is normally a large fraction of the building refurbishment cost.

The main goals of this work were to model, assess and propose a retrofitting solution for a RC building considered as representative of the building stock designed and built between 1960 and 1980 in Portugal. For this, nonlinear static (pushover) analyses, using the structural analysis software SAP2000 (CSI, 2016), in order to fulfil the seismic performance required in Part 3 of Eurocode 8 [4] were used. This study starts with a brief description of the building chosen as a case study (§ 2). Afterwards, a brief review of the main modelling strategies is presented (§ 3). Then, the seismic assessment of the building based on the extended N2 procedure is performed and the results are discussed (§ 4). A Brief review of the design and seismic assessment of retrofitting strategy is present in § 5. Finally, in § 6 is presented the final considerations of this study.

2. OVERVIEW OF THE CASE STUDY

The case of study in this dissertation is an eight-storey concrete building (figure 1), located in Lisbon (Portugal), with a frame-wall horizontal resisting system that can be considered as a representative example of buildings built between 1960 and 1980 in the city. Its plan dimensions are 36.60m in the X-direction and 10.85m in the Y-direction. Total building height is 27m.

Figure 1-Case study building

These RC buildings, of 8 to 12 floors, have the following distinctive characteristics:

(i) Wall-frame horizontal resisting system;
(ii) With an open ground storey and infills in the upper storeys (pilotis type building);
(iii) Columns mainly oriented in one direction;
(iv) Eccentric RC core walls (stair cases);
(v) Smooth reinforcement bars.

The building was design by the civil engineer Luiz do Pilar in 1960, and belongs to a first generation of buildings design for resist to earthquakes (RSCCS [1]). However, this first generation of seismic resistance codes, based on simplified design method and unrealistic seismic acceleration evaluation, combine with several inadequate structural design options, lead in general to a poor seismic performance of the building. Due to an inadequate seismic design, this particular representative building was addressed in several seismic analyses, namely [5], [6] and [7].

I. Structural characterization

The structure was design as frame system, featuring three main RC frames, for the vertical and horizontal loads in the longitudinal direction (X direction) and with a resisting walls system for horizontal loads in the transversal direction (Y direction), located in the two stairs and lift cores (Figure 2). The wall systems feature two rectangular walls, with 4,0x0,25m and two T-section walls with an additional 3,0x0,15m member in the longitudinal direction of the building. In fact, the rigidity of the T-Section walls in both directions should have significant impact on the seismic response of the structure in both directions.

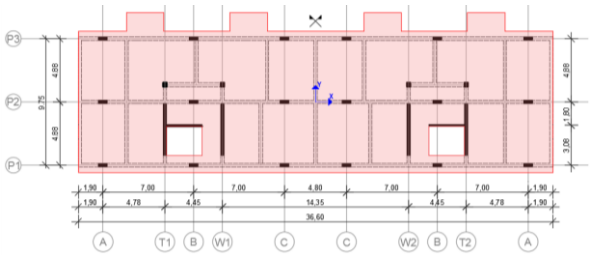

Figure 2 – Identification of element at the floor level

It should be notice some irregularities in elevation, namely:

(i) the discontinuity of the infill walls at the ground floor which can lead to a soft-storey mechanism;
(ii) the reduction of the column section in each floor.

Moreover, in term of reinforcement detailing, some inadequate conditions were identified, namely:

(i) The spacing and number of the columns' transverse reinforcement ties is generally insufficient, originating the premature failure of the section due to shear and buckling of the bars under compression. Furthermore, the distance between consecutive longitudinal bars restrained by ties exceeds the EC8-1 limit (200 mm);
(ii) RC elements are characterized by smooth longitudinal reinforcing bars, which increase the bond-slip effect.
(iii) According to modern standards, such as Part 1 of EC2 [9] and Part 1 of EC8, to ensure a ductile behaviour of the RC walls, the reinforcement details should be characterized by confined boundary elements and adequate levels of horizontal ratios. However, RC walls designed according to older codes, such as the case study, do not feature these characteristics.

3. COMPUTATIONAL MODELLING OF THE BUILDING

The 3D model of the studied building was developed using SAP2000 (CSI, 2016), which allows different types of analysis. The ones used in this study were modal analysis for the dynamic characterization of the structure, response spectrum analysis, for the application of extended N2 method and nonlinear static ("pushover") analysis based on the procedure described in EC8 (N2 method).

I. Materials

The materials adopted for the RC structure (beams, columns, slabs, shear walls and footings) in accordance with the original drawings are the S235 steel with smooth plain rebars and the B25 (C20/25) concrete. Regarding the retrofitting solution, the same C20/25 concrete and the S500 steel with ribbed rebars were adopted.

Steel

S235 is a mild steel which properties were specified in the old national standards (e.g. REBAP and RSA) in terms of the main parameters: yield strength, ultimate strength and strain When compared to the current properties of reinforcing steel (typically S400 or S500), the difference lies mainly in the required ductility. The main properties assumed were as follows in Table 1.

Table 1 – Properties of S235 and S500 steel considered.

Mild Steel	S235	S500 NR
Modulus of Elasticity (GPa)	210	210
Poisson's Ratio	0.30	0.30
Yield strength (MPa)	235	500
Minimum ultimate strength (MPa)	360	500
Yield strain	0.00112	0.00238
Hardening strain	0.01500	–
Minimum strain at breaking	0.24000	0.06750

The model proposed by Park and Paulay (1975) was adopted as the constitutive relation for S235 steel, defined in Figure 3, since the S235 steel is characterized by a high hardening rate in the plastic stage. Regarding the S500 steel was adopted a bilinear stress-strain relationship.

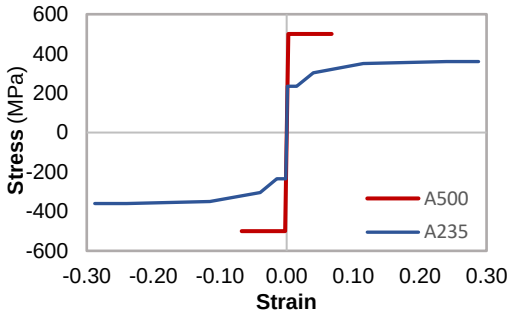

Figure 3 – Stress-strain diagram for steel.

Concrete

Due to an inadequate detailing of the transverse reinforcement on the RC members, it was assumed for the original model a stress-strain relationship of an unconfined concrete. In the retrofitting solution presented in this work, it was assumed for confined concrete a constitutive relation based on the theory proposed by Mander et al. (1988). The main properties of the adopted confined and unconfined C20/25 concrete are as follows in Table 2.

Table 2 – Properties of C20/25 concrete considered.

Concrete	*C20/25 Unconfined*	*C20/25 Confined*
Tangent *Modulus of Elasticity* (GPa)	31.5	31.5
Poisson's Ratio	0.20	0.20
Mean value of tensile strength (MPa)	2.2	2.2
Compressive strength (MPa)	28.0	32.1
Compressive strain at peak	0.0020	0.0034
Ultimate strain	0.0035	0.0070

The confined concrete stress-strain relation, presented in figure 4, was defined for the confined boundaries elements of the T-section walls for the strengthening solution.

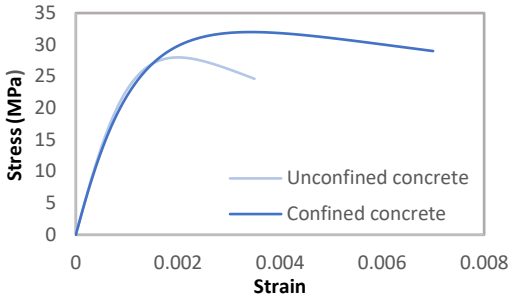

Figure 4 – Stress-Strains relations for confined and unconfined concrete.

II. Modelling of structural and non-structural elements for linear analysis

The columns and beams of the case study building were modelled as linear, horizontal and vertical, frame elements of C20/25 concrete. The cross-sections were modelled with SAP2000 Section Designer (CSI, 2009). The same strategy was considered for the modelling of RC walls. The lightened slabs were modelled with thick shell elements of C20/25 concrete, with a reduction of the thickness, determined to ensure that the mass per unit volume and the rigidity of the material are similar to the properties of the original slab.

Regarding the foundation, from original drawing of the project [8], one can notice that the columns were design as pinned at the base. Therefore, the columns were modelled at the base just with restrained translations in all directions (X, Y and Z). Regarding foundation of the RC walls, as a conservative approach in terms of evaluation of seismic effects, the rotation restrains at the base, in both X and Y direction of the T-walls and around the strong axis of the longitudinal direction of rectangular walls, were considered as fully rigid.

The infill walls were modelled considering the simplify method, proposed on [9], by means of two diagonal struts which can only carry loads in compression, placed between the beam–column joints.

III. Nonlinear modelling strategy

Inelastic behaviour can be modelled by several different ways. There are two main groups of modelling strategies: concentred plasticity models, with inelastic behaviour concentred at elements extremities, through the application of rigid-plastic hinges (Figure 5a) or an inelastic spring hysteretic properties (Figure 5b) or distributed plasticity models namely with fibre-based models (Figure 5d) and finite element models (Figure 5e) [10].

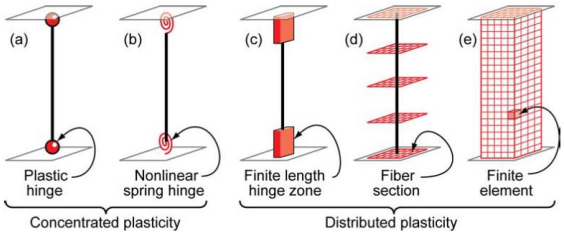

Figure 5 – Idealized models of beam-column elements (adapted from [10]*)*

According to [11] the concentred plasticity models were originally developed for frame analysis, for which the assumption of localised inelastic deformations in columns and beams at their extremities holds reasonably close to their real behaviour. On the other hand, for walls the hinge length is around the storey height. Therefore, concentration of inelastic deformations in a single plastic hinge at the wall base does not represent correctly the deformation behaviour at the first storey. Therefore, in this work it was considered the following inelastic modelling strategies:

For beams and columns: model with concentrated the inelastic deformations at the elements' extremities, such as through a plastic hinge;

RC walls: model with distributed plasticity through the application of fibre section along the member length.

Modelling of nonlinear behaviour of beams and columns

In this work, the nonlinear modelling of the beams and columns used was developed in [5] through the implementation of manually defined plastic hinges at the elements extremities. For beams section was considered only one relationship considering the bending moment M3. For columns was considered plastic hinges with an interaction P-M2-M3 relationship, defined for each different section and axial force.

Regarding the definition of the plastic hinge length L_p, it was considered the empirical expression (1) proposed by Paulay and Priestley [12], with a reduction of 50% for taking into account the effect of smooth plain rebars.

$$L_p = 0.08l + 0.022 f_{sy} d_{bl} \qquad (1)$$

Where l is the length of the RC element, d_{bl} is the diameter of the main longitudinal reinforcing bars, and f_{sy} is the yielding strength of the reinforcement (in MPa).

Modelling of nonlinear behaviour of RC walls

For modelling of nonlinear behaviour of RC walls was adopted a fiber-based nonlinear model, with fiber section distributed along the elements (Figure 5d). To assess the influence of fiber discretization at the cross-section level and of the distribution along the element a sensitivity analysis was performed.

Modelling of nonlinear behaviour of infill walls

In this work, the nonlinear behaviour of the infill walls was considered by means of concentrated plastic hinge with an axial force-displacement relationship, based on modelled proposed at [13].

4. SEISMIC ASSESSMENT OF THE EXISTING RC STRUCTURE

To assess the seismic capacity of the structure, nonlinear static analyses were performed based on the N2 method proposed by Fajfar [14] and prescribed in EC8-3 [4]. The effect of the higher modes both in plan and elevation was considered by the extend N2 method proposed on [15] and [16].
The seismic assessment was performed by comparing the demand with the capacity at the significant damage (SD) limit state, as prescribed by the Portuguese National Annex of EC8-3[4], with an return period of 475 years for the seismic action.

Ductile component

According to EC8-3 [4], the seismic assessment of ductile components/mechanism of the structural elements is performed in terms of chord rotation capacity θ_{um}, defined as the angle between the tangent to the axis at the yielding end and the chord connecting that end with the end of the shear span (L_V = M/V = moment/shear at the end section), i.e., the point of contraflexure.
From the result obtain on the pushover analyses, the chord rotation was calculated based on the following expression, proposed on [17]:

$$\theta = \chi_y \frac{L_v}{3} + (\chi - \chi_y) L_{pl} \left(1 - \frac{L_{pl}}{2L_v}\right) \qquad (2)$$

where χ is the curvature obtains from the analysis; χ_y is the yield curvature of the section, L_{pl} is the plastic hinge length and L_v is the shear span or ratio moment/shear at the end section.

The ultimate chord rotation capacity, may be calculated, according to [4], from the following expression:

$$\theta_{um} = \frac{1}{\gamma_{el}} \left[0{,}016(0{,}3^{\upsilon}) \left[\frac{máx(0{,}01;\omega')}{máx(0{,}01;\omega)} f_c\right]^{0{,}225} \cdot \left(\frac{L_v}{h}\right)^{0{,}35} 25^{\left(\alpha\rho_{sx}\frac{f_{yw}}{f_c}\right)} (1{,}25^{100\rho_d}) \right] \qquad (3)$$

where γ_{el} is equal to 1.5, υ is the normalized axial force, h is the depth of cross section, L_v is the shear span or ratio moment/shear at the end section, ω and ω' are the mechanical reinforcement ratio of the tension and compression longitudinal reinforcement, respectively, f_c and f_{yw} are the concrete compressive strength and the stirrup yield strength, respectively, ρ_{sx} is the ratio of transverse steel parallel to the direction x of loading, ρ_d is the steel ratio of diagonal

reinforcement and α is the confinement effectiveness factor. For member with smooth longitudinal bars, the EC8-3 [4] provide a correction coefficient of 0.575 for the value of the ultimate chord rotation capacity calculated according to the expression (3).
The chord rotation capacity corresponding to SD limit state (θ_{SD}) is taken as 3/4 of the ultimate chord rotation θ_{um}, as prescribed by EC8-3.

Brittle component

The shear resistance of the elements was evaluated by mean of cyclic shear resistance V_R, prescribed by EC8-3 [4], and by shear strength V_n, defined in the ATC-40 norm [18]. Concerning the RC walls, was also evaluated the shear resistance corresponding to web crushing $V_{Rd,\,max}$.

I. N2 Method

Figure 6 and 7 shows the pushover capacity curves for the X direction (model with and without the presence of masonry infill) and Y direction, with their respective target displacements, calculated from N2 methods proposed on EC8-3 (and considering the reduce and unreduced seismic design action). The curves represent the base shear against the displacement at the center of mass of the top floor. One can observe the increase of resistance and stiffness with the consideration of infills, which can explain the reduction of the target displacement in the X analysis with the wall-frame resisting system. However, the inadequate relation between ductility and strength, lead to an earlier collapse of the structure, with the ductile failure of the RC walls (ensure 65% of the base shear in X direction), without reaching the target displacement. This can be explained with an inadequate ductile detailing of the walls, leading to the failure of the unconfined concrete on the web of the RC walls. It is important to note that, due to the symmetry of the building, the seismic response on the X+ direction and X- direction is similar.

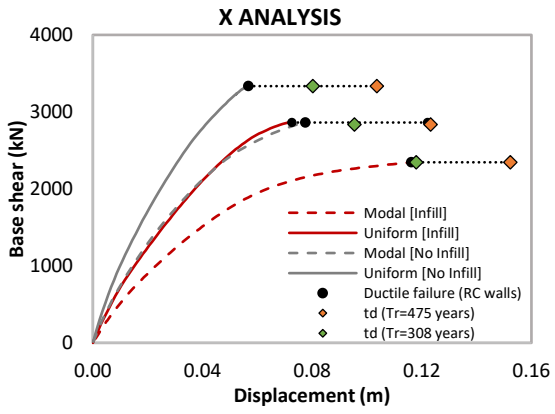

Figure 6 - Capacity "pushover" curves in X direction (original model)

Regarding the Y analysis (Figure 7), the wall-system featuring the 4 RC walls, show a higher resistance and deformation capacity comparing with the wall-frame system in the X direction. Therefore, the structure reaches the target displacement before the failure of the critical RC wall.

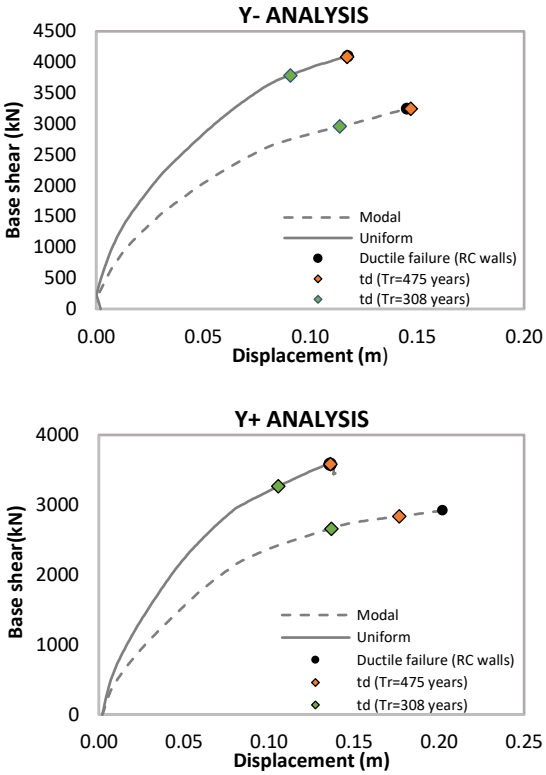

Figure 7 – Capacity "pushover" curves in Y direction (original model)

II. Extended N2 Method

The extended N2 method, was developed for considering higher mode effects both in plan [15] and in elevation [16] by means of a correction factors, applied to the relevant results of the pushover analysis. This simplified conservative method, is based on assumption that the structure remains in the elastic range when vibrating in higher modes. The procedure for determining the correction factors both in plan (c_p) and elevation (c_{ed} for displacement and c_{er} for storey drift) combines the results from the nonlinear static (pushover) analysis with the results from a response spectrum analysis with the consideration of all the relevant vibration modes. For the response spectrum analysis, was considered an alternative model with a rigid diaphragm, considering an accidental eccentricity of 5% of the building length in each direction. According to [16], both factors in plan and elevation are compatible. Therefore, for evaluation of inter-storey drifts, the two correction factors could be combined in a single factor c_F.

$$c_F(x,y,z) = c_p(x,y) \cdot c_{er}(z) \qquad (4)$$

The correction facto c_F is applied to for internal forces and deformation of the elements.

I. Analyse of results

Considering the extended N2 method, with the consideration of the higher modes in plan and elevation, the maximum inter-storey drift ratios of the structure are shown in Figures 8 and 9 for the X direction at the ultimate displacement and Y direction at the target displacement, respectively. In the X direction, the maximum inter-storey drift ratios are reached at the 4th floor, for a value of 0.44 %. The effect of the irregularity in elevation on the inter-storey drift, due to the consideration of the infill, can be noticed with the reduction between the ground floor and the 1st floor, intensified by the pinned foundation of the columns.

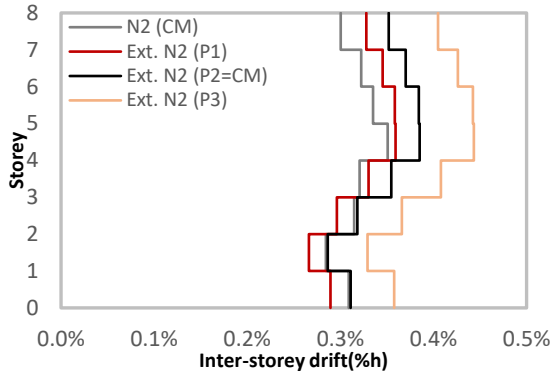

Figure 8 – Maximum Inter-storey drift ratio at the ultimate displacement in the X direction.

Regarding the Y direction, it can be seen a maximum inter-storey drift ratio of 1.04%, reached at the 6th floor. Considering as reference the damage limitation requirement of the EC8-1 [19], which prescribe a maximum inter-storey drift ratio of 1.25%h (considering reduction factor υ=0.4 which takes into account the lower return period of the seismic action) for buildings with brittle non-structural elements attached to the structure, the values verified for the study case are very reasonably. This level of displacements' control is possible due to the contribution of the stiffness of the RC walls.

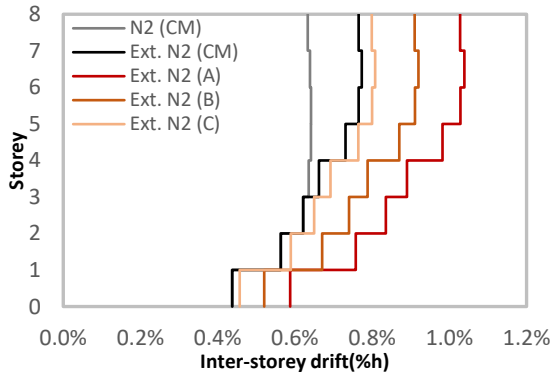

Figure 9 - Maximum Inter-storey drift ratio at the target displacement in the Y direction.

Figure 10 shows the trend for the columns to form plastic hinges, mainly on the upper floors, while mostly at the bottom storeys, the formation of plastic hinges occurs in the beams. In fact, in the bottom floors the moment resistant of the columns is substantially superior due to the larger section and the larger value of axial load. In the other hand, the cross section of the beams remains unchanged in elevation. This configuration at the top floors, with the inelastic behaviour occurring mainly on the columns, can lead to a storey mechanism, with lower energy dissipation capacity. The collapse was just avoided due to the contribution of the RC walls, which confers redundancy to the structural system.

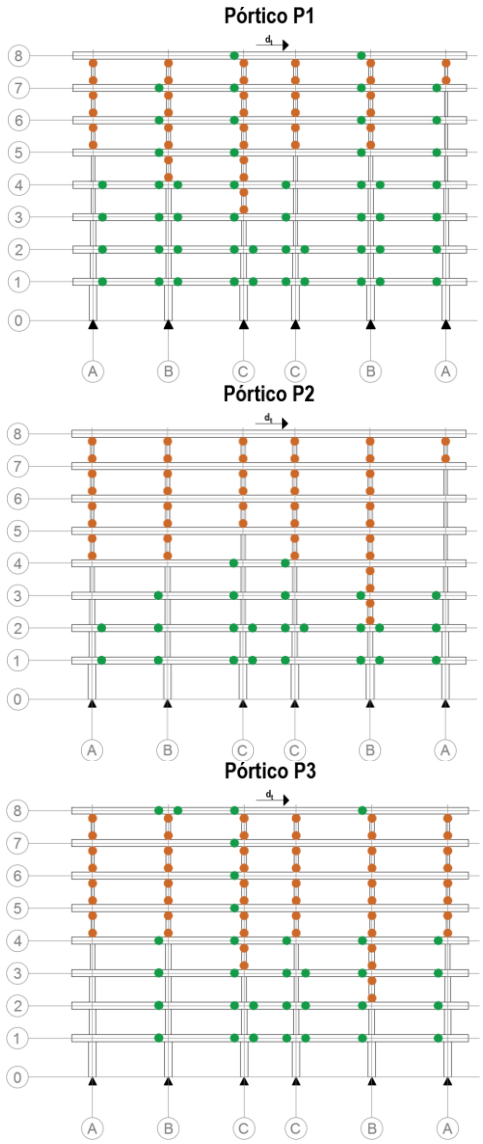

Figure 10 - Limit State of the hinges for X analysis for the ultimate displacement.

Regarding the soft-storey mechanism at the ground floor level, one can notice that the columns do not reach the yielding. This fact can be justified with the pinned connection at the base of the columns, which lead to a significant decreasing of the rigidity and therefore, lower internal forces for the imposed displacement. This flexible behaviour explains the lower ratio between chord rotation of the columns and the ultimate chord rotation capacity defined by the

EC8-3[4] for the columns, presented in Table 3 (where DL correspond to Damage Limitation state), for the extended N2 method. However, it is important to note that the displacement for which the columns were evaluated do not correspond to the target displacement, once that the structure collapse earlier in the X direction with the ductile failure of the T-walls.

Table 3 – Limit states (ductile) of each column for the most unfavourable case (extended N2 method).

		Extension of N2 method					
Column		Frame P1		Frame P2		Frame P3	
		$\theta/\theta_{u,s}$	LS	$\theta/\theta_{u,s}$	LS	$\theta/\theta_{u,s}$	LS
A	0	10%	DL	6%	DL	15%	DL
	1	19%	SD	14%	DL	19%	DL
	2	25%	SD	19%	SD	34%	DL
	3	42%	SD	43%	SD	42%	SD
	4	50%	SD	67%	SD	52%	SD
	5	38%	SD	61%	SD	49%	SD
	6	35%	SD	58%	SD	41%	SD
	7	34%	SD	44%	SD	31%	SD
B	0	10%	DL	8%	DL	19%	DL
	1	13%	SD	11%	DL	20%	DL
	2	19%	SD	18%	DL	33%	DL
	3	23%	SD	22%	SD	34%	SD
	4	34%	SD	24%	SD	39%	SD
	5	34%	SD	24%	SD	37%	SD
	6	29%	SD	23%	SD	33%	SD
	7	26%	SD	21%	SD	24%	SD
C	0	12%	DL	9%	DL	11%	DL
	1	22%	DL	13%	DL	19%	DL
	2	31%	SD	23%	DL	32%	SD
	3	37%	SD	30%	SD	37%	SD
	4	41%	SD	42%	SD	42%	SD
	5	47%	SD	33%	SD	40%	SD
	6	36%	SD	27%	SD	32%	SD
	7	35%	SD	32%	SD	26%	SD
$\frac{\sum \theta/\theta_{u,s}}{n}$		29%		28%		32%	

As mentioned before, the structure components must be verified for potential brittle mechanism that could lead to a premature collapse of the structure.

Table 4 - Limit states (brittle) for of each column for the most unfavourable case (EC8-3).

		Extension of N2 method					
Column		Frame P1		Frame P2		Frame P3	
		V_2/V_r	LS	V_2/V_r	LS	V_2/V_r	LS
A	0	80%	DL	98%	DL	75%	DL
	1	147%	NC	178%	NC	104%	NC
	2	166%	NC	243%	NC	122%	NC
	3	204%	NC	235%	NC	158%	NC
	4	211%	NC	213%	NC	165%	NC
	5	240%	NC	242%	NC	178%	NC
	6	259%	NC	256%	NC	182%	NC
	7	245%	NC	245%	NC	192%	NC
B	0	60%	DL	208%	NC	81%	DL
	1	110%	NC	403%	NC	119%	NC
	2	139%	NC	419%	NC	137%	NC
	3	179%	NC	396%	NC	148%	NC
	4	186%	NC	245%	NC	139%	NC
	5	206%	NC	281%	NC	148%	NC
	6	215%	NC	305%	NC	155%	NC
	7	212%	NC	214%	NC	164%	NC
C	0	68%	DL	81%	DL	57%	DL
	1	119%	NC	133%	NC	94%	DL
	2	138%	NC	169%	NC	115%	NC
	3	160%	NC	223%	NC	129%	NC
	4	160%	NC	187%	NC	131%	NC
	5	185%	NC	219%	NC	145%	NC
	6	203%	NC	258%	NC	158%	NC
	7	220%	NC	191%	NC	166%	NC

Table 4 shows that the evaluation of the shear resistance according to the EC8-3[4] (where NC correspond to Near Collapse limit state) lead to a brittle failure of mostly every column of the frames. On the other hand, an evaluation of the shear resistance based on ATC-40 [18] leads to a significant large values of shear resistance (Table 5), with brittle failure occurring mostly between the 1st and 3rd floors.

Table 5- Limit states (brittle) for of each column for the most unfavourable case (ATC-40).

		Extension of N2 method					
Column		Frame P1		Frame P2		Frame P3	
		V_2/V_r	LS	V_2/V_r	LS	V_2/V_r	LS
A	0	34%	DL	44%	DL	36%	DL
	1	90%	DL	131%	NC	70%	DL
	2	84%	DL	157%	NC	69%	DL
	3	107%	NC	129%	NC	87%	DL
	4	83%	DL	89%	DL	68%	DL
	5	88%	DL	95%	DL	73%	DL
	6	84%	DL	91%	DL	68%	DL
	7	65%	DL	74%	DL	51%	DL
B	0	25%	DL	65%	DL	41%	DL
	1	57%	DL	176%	NC	77%	DL
	2	77%	DL	179%	NC	102%	NC
	3	91%	DL	154%	NC	104%	NC
	4	83%	DL	79%	DL	78%	DL
	5	84%	DL	80%	DL	80%	DL
	6	76%	DL	76%	DL	75%	DL
	7	60%	DL	46%	DL	61%	DL
C	0	31%	DL	39%	DL	27%	DL
	1	76%	DL	101%	NC	64%	DL
	2	72%	DL	112%	NC	64%	DL
	3	80%	DL	116%	NC	73%	DL
	4	61%	DL	76%	DL	54%	DL
	5	73%	DL	86%	DL	60%	DL
	6	70%	DL	92%	DL	56%	DL
	7	59%	DL	59%	DL	46%	DL

Considering the shear resistance based on ATC-40 [18], one can observe by comparing the bending and shear behaviour of the columns that at the upper storeys the failure should be caused by the reaching the total chord rotation capacity of the section, while the shear force is limited by the resisting bending moment. On the other hand, between the 1st and 3rd floors, results indicate that the columns could suffer a brittle failure, namely on the central frame (P2) due to higher reinforcement ratios. This can be justified by the higher resisting moment verified at the lower storeys with the increase of the cross-section and axial load, while the transverse reinforcement remains the same.

Table 6 show the state of the T-walls, in terms of rotation, for the most unfavourable case in the X-direction. Due to the symmetry of the T-walls, one can observe a significant difference between the two walls, with T1 subjected to a negative bending moment (with compression on the web) and T2 subjected to a positive bending moment (with compression on the flange). This difference leads to a significant higher resistance and lower chord rotation capacity for the wall with the compressed web, with the collapse occurring due to reaching of the unconfined ultimate strain of concrete. The opposite wall shows a significant rotation capacity, with the compressions along the flange length, exploring all the ductility of the web's longitudinal reinforcement.

Table 6 – T-wall limit states for X+ analysis

Wall	c_F	N $[KN]$	M_2 $[KNm]$	θ_2 $[rad]$	$\theta_{2,DL}$ $[rad]$	$\theta_{2,NC}$ $[rad]$	LS
T1	1.04	2733	-7531	-0.0063	-0.0033	-0.0046	X
T2	1.04	2750	2129	0.0060	0.0020	-0.0105	SD

X - Failure

Regarding the Y direction, the four walls present a similar behaviour (Table 7). Therefore, for the target-displacement, considering the correction of the extended N2 method and the effect of the smooth rebars, one can observe that the chord rotations for the four walls reach the ultimate capacity.

Table 7 - RC wall limit states for Y analysis

Wall	c_F	N $[KN]$	M_2 $[KNm]$	θ_2 $[rad]$	$\theta_{2,DL}$ $[rad]$	$\theta_{2,NC}$ $[rad]$	LS
T1	1.25	2118	5928	0.0090	0.0023	0.0090	NC
W1	1.15	2111	6223	0.0092	0.0024	0.0092	NC
W2	1.15	2205	6248	0.0091	0.0024	0.0092	NC
T2	1.25	2281	6627	0.0086	0.0023	0.0089	NC

Nevertheless, for the shear resistance defined according to the EC8-3[4], it was possible to conclude that the RC walls should suffer a brittle failure before reaching the ultimate rotation capacity.

5. SEISMIC RETROFITTING

The main goal of the seismic retrofitting strategy for the study case of this work was the correction of the rotation capacity of the T-wall, which is the cause for the premature collapse of the building in the longitudinal direction. The solution showed on Figure 11 consists of a concrete jacketing with a partial demolition of the T-wall's web and reconstruction of the confined boundary element, to increase the rotation capacity. To ensure the ductile failure mode of the walls a transverse reinforcement was accommodate on concrete jackets.

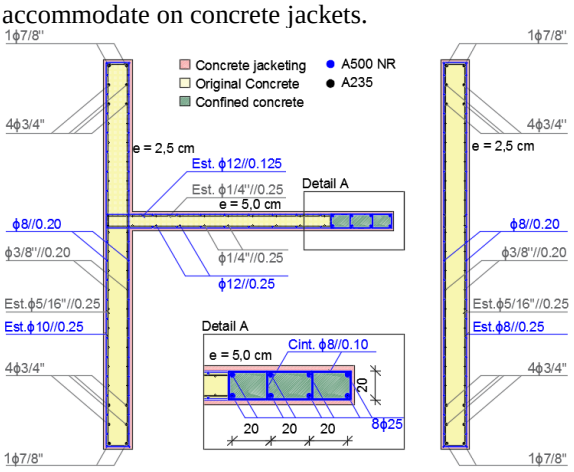

Figure 11 – Retrofitting solution the RC-walls

Figure 12 shows the effect of retrofitting of the walls on the pushover curves for the X direction, with a significant increase of the deformation capacity of the structure, mostly due to a higher value of ultimate strain of the confined concrete.

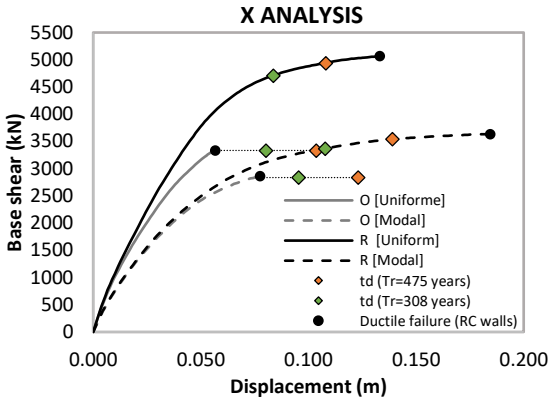

Figure 12 - Capacity "pushover" curves in X direction (O- original and R-retrofit model)

Table 8 shows the limit state of the T-walls for the seismic action on X direction. One can observe the significant increase of the rotation capacity of the walls subjected to negative bending moment (compression at the web) due to the confinement of the concrete at the confined concrete element. On the other hand, for the positive bending moment (compression at the flange) it is shown a significant higher value of moment resistance, but with a reduction of the rotation capacity. In terms of limit state verification, it is noticed that for the target-displacement, the critical wall is sufficiently closed to the rotation limit of the near collapse limit state without considering the seismic reduction prescribed on EC8-3[4].

Table 8 - T-wall limit states for X+ analysis (retrofit)

Wall	c_F	N $[KN]$	M_2 $[KNm]$	θ_2 $[rad]$	$\theta_{2,SD}$ $[rad]$	$\theta_{2,NC}$ $[rad]$	LS
T1	1.04	-2746	7130	0.0053	0,0070	0,0093	NC
T2	1.04	-2992	-14663	-0.0046	-0,0105	-0,0141	SD

In terms of the limit state of the frame´s columns (Table 9), even with a significant higher displacement (on the analysis the frames were assessed for an ultimate displacement value lower than the target displacement) due to a significant lower stiffness of the frames with the soft -story mechanism devolving at the upper storey, the main difference notice was an increase of rotation of the columns. In fact, due to the increasing of the torsion effect, in order to fulfil the SD limit state of the P3 frame, it was necessary to consider the reduction of the seismic action.

Regarding the shear verification, the same general conclusion was reached, with the need for retrofitting almost all the columns, for the shear strength defined by EC8-3[4] (Table 4). When the shear resistance is defined according to the ATC-40 norm [18], only the columns between the 1st and 3rd need retrofitting (Table 5). For the shear strengthening, the solution proposed in this work was the Carbon-Fibre Reinforced Polymer (CFRP), which are simply and fast to apply. This fact can have higher impact on

intervention's cost, especially in cases with a need for intervention on a significant number of structural elements.

Table 9 – Limit states (ductile) of each column for the most unfavourable case (retrofit model).

Column		Extension of N2 method					
		Frame P1		Frame P2		Frame P3*	
		$\theta/\theta_{u,s}$	LS	$\theta/\theta_{u,s}$	LS	$\theta/\theta_{u,s}$	LS
A	0	4%	DL	5%	DL	10%	DL
	1	20%	*SD*	11%	DL	18%	DL
	2	31%	*SD*	22%	DL	38%	DL
	3	33%	*SD*	31%	*SD*	44%	*SD*
	4	39%	*SD*	42%	*SD*	53%	*SD*
	5	40%	*SD*	40%	*SD*	52%	*SD*
	6	41%	*SD*	60%	*SD*	48%	*SD*
	7	48%	*SD*	54%	*SD*	38%	*SD*
B	0	8%	DL	6%	DL	15%	DL
	1	15%	*SD*	11%	DL	19%	DL
	2	22%	*SD*	15%	DL	35%	DL
	3	21%	*SD*	47%	*SD*	43%	*SD*
	4	35%	*SD*	49%	*SD*	51%	*SD*
	5	42%	*SD*	52%	*SD*	52%	*SD*
	6	43%	*SD*	53%	*SD*	46%	*SD*
	7	43%	*SD*	51%	*SD*	33%	*SD*
C	0	10%	DL	8%	DL	11%	DL
	1	20%	DL	14%	DL	20%	DL
	2	31%	*SD*	24%	DL	35%	*SD*
	3	33%	*SD*	30%	*SD*	49%	*SD*
	4	36%	*SD*	39%	*SD*	63%	*SD*
	5	42%	*SD*	39%	*SD*	63%	*SD*
	6	38%	*SD*	58%	*SD*	51%	*SD*
	7	28%	*SD*	53%	*SD*	36%	*SD*
$\frac{\sum \theta/\theta_{u,s}}{n}$		**30%**		**34%**		**39%**	

Regarding the Y direction, on can observe the increased stiffness with the concrete jacking of the walls (Figure 13), with a possible reduction of the target displacement. Therefore, Table 10 shows a limit state verification with some additional safety.

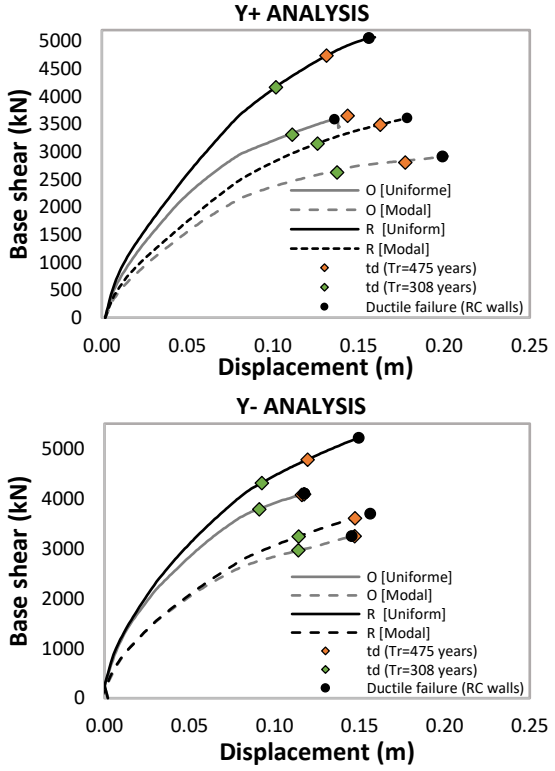

Figure 13- Capacity "pushover" curves in Y direction (O-original and R-retrofit model)

Table 10 - wall limit states for X+ analysis (retrofit)

Wall	c_F	N $[KN]$	M_2 $[KNm]$	θ_3 $[rad]$	$\theta_{3,SD}$ $[rad]$	$\theta_{3,NC}$ $[rad]$	LS
T1	1.25	-2775	13901	0.0064	0,0107	0,0143	*SD*
W1	1.15	-2762	10353	0.0085	0,0122	0,0163	*SD*
W2	1.15	-2879	7061	0.0063	0,0117	0,0154	*SD*
T2	1.25	-2837	9789	0.0044	0,0103	0,0136	*SD*

On Table 10 it also can be observed the effect of the torsion on the results of non-linear static analyses, leading to the higher values of bending moment and rotation of the T1 and W1 walls. This effect was caused by the retrofitting solution, which lead to an increase of the building asymmetries, causing an increasing of torsion at the fundamental mode on the X direction, considered for the modal load pattern.

Table 11 – Shear verification

Wall		ρ_w (%)	c_F	N $[KN]$	V_{Ed} $[KN]$	V_R $[KN]$	$V_{Rd,max}$ $[KN]$	LS
W	**web**	0.27	1.15	-2476	1103	1342	3397	*DL*
T	**flange**	0.35	1.25	-2325	1645	1678	3397	*DL*
	web	0.83	1.05	-2992	2098	2539	2301	*DL*

Table 11 shows the shear strength verification for the proposed solution (Figure 11). Due to a higher bending moment resistance of the T-walls with the contribution of the flange's reinforcement, it was needed a consideration of a significantly higher transverse reinforcement on concrete jacket of the T-wall's webs, in order to the SD limit state (which is corresponded to the same requirement of the DL limit state for shear verification). Whit the increasing of the shear resistance controlled by the stirrups $V_{R,}$ it can be observed that shear strength of the T-walls is now conditioned by the maximum shear resistance corresponding to web crushing $V_{Rd,max}$.

6. FINAL CONSIDERARIONS

An eight-storey RC building, located in Lisbon and built in the 1960's, was studied in this research. With a preliminary assessment of the structure some inadequate reinforcement detailing conditions and irregularity in elevation were noticed.

From the nonlinear static pushover analysis performed for the 3D computational model developed using SAP2000 (CSI, 2016) the main deficiencies were identified. It was possible to concluded that the critical element in terms of ductile components of the structure are the RC walls, which present an inadequate relation between strength and ductility, leading to a premature collapse of the structure. Nevertheless, it was possible to conclude that, according to the EC8-3[4], the walls should suffer a brittle failure before reaching the ultimate rotation capacity.

In terms of the resisting frames, the general conclusion was an inefficient performance for lateral force resisting system, due to an inadequate design for

seismic resisting, mainly due to a formation of soft-storey mechanism at the upper floor due to the yelling of the columns at the nodes, leading to a significant reduction of the frames stiffness. Regarding the shear verification, a comparison between the EC8-3[4] and the ATC-40[18] was performed. The EC8-3[4] leads to a significant lower values of the shear capacity, with the conclusion that the columns should suffer a brittle failure before reaching the resisting bending moment.

The retrofitting solution proposed, based on the results of the nonlinear static pushover analyses, in terms of ductile behaviour, was able to fulfil the performance requirement of EC8-3 [4], with a relatively located intervention at the 1st and 2nd floors of the RC walls, by means of a concrete jacketing, with the reconstruction of the confine elements at the t-wall´s webs. Namely with the increasing of the confined concrete's ultimate strain on the confine boundary elements, it was possible to improve significantly the deformation capacity of the structure and fulfil the SD limit state defined as the goal for this work. Regarding the shear resistance of the walls, a transverse reinforcement accommodated at the concrete jacketing was designed to ensure that brittle failure does not occur.

Regarding the shear strengthening of the frame's columns, a solution with CFPR was proposed, and evaluated with consideration of two different alternatives (EC8-3[4] and the ATC-40[18]). Considering the shear resistance prescribed by the EC8-3[4], in order to fulfil the SD limit state it is necessary a retrofitting of all the column's above the ground floor. On the other hand, according to the expression for the shear resistance of ATC-40 [18], the critical columns in terms of brittle failure are located between the 1st and the 3rd floor, where the resistant moment are higher. Above the 3rd floor, where a general reduction of the cross section occurs, the maximum shear stress corresponding to the resistant moment should be lower than the shear resistance, which prevent a brittle failure of the columns. This significant difference, with greater impacts on the retrofitting solutions for existing structures, should be addressed in future studies.

7. REFERENCE

[1] Ministério das Obras Publicas (1958) *Regulamento de Segurança das Construções contra os Sismos*.

[2] J. Saraiva e J. Appleton (2006) *Avaliação Da Capacidade Sísmica De Edifícios De Betão Armado De Acordo Com O Eurocódigo 8 – Parte 3*.

[3] Ministério da Habitação, Obras Publicas e Transportes (1983) *Regulamento de Estruturas de Betão Armado e Pré-Esforçado*.

[4] EN 1998-1-3 (2004) *Eurocode 8: Design of structures for earthquake resistance - Part 3: Assessment and retrofitting of buildings*

[5] D. Santos (2016) *Seismic Assessment and Retrofitting of an old Reinforced Concrete Building in the city of Lisbon*.

[6] P. Lamego (2014) *Reforço sísmico de edifícios de habitação. Viabilidade da mitigação do risco*.

[7] C. Caruso, R. Bento, J. M. Castro, e E. M. Marino (2017) *Seismic Performance Assessment of Old Frame-Wall Buildings in Lisbon.*

[8] Montepio-Geral (1960) *Peças Desenhadas do Porjecto de Edifício sito na Avenida do Brasil, Lote 6, Bloco A e B. Lisboa*.

[9] R. J. Mainstone (1971) *On the stiffnesses and strengths of infilled frames*.

[10] G. G. Deierlein, A. M. Reinhorn, e M. R. Willford (2010) *Nonlinear Structural Analysis For Seismic Design: A Guide for Practicing Engineers.*

[11] K. Beyer, S. Simonini, R. Constantin, e A. Rutenberg (2014) *Seismic shear distribution among interconnected cantilever walls of different lengths*.

[12] T. Paulay e M. Priestly (1992) *Seismic Design of Reinforced Concrete and Masonry Buildings*.

[13] M. Dolšek e P. Fajfar (2008) *The effect of masonry infills on the seismic response of a four-storey reinforced concrete frame.*

[14] P. Fajfar e M. Fischinger (1988) *N2 - A Method for Non-Linear Seismic Analysis of Regular Buildings.*

[15] P. Fajfar, D. Marusic, e I. Perus (2005) *Torsional Effects in the Pushover-Based Seismic Analysis of Buildings.*

[16] M. Kreslin e P. Fajfar (2011) *The extended N2 method taking into account highermode effects in elevation.*

[17] M. Fardis (2009) *Seismic design, assessment and Retrofitting of concrete Buildings*.

[18] ATC (1996) *ACT-40 : Seismic Evaluation and Retrofit of Concrete Buildings, volumes 1 and 2*.

[19] NP EN 1998-1-1 (2010) Eurocódigo 8: Projecto de estruturas para resistência aos sísmos - Parte 1: Regras gerais, acções sísmicas e regras para edifícios.